Nanoscale Res Lett (2010) 5:818–822
DOI 10.1007/s11671-010-9566-5

NANO EXPRESS

Localized Surface Plasmon Resonance Biosensing with Large Area of Gold Nanoholes Fabricated by Nanosphere Lithography

Gansheng Xiang · Nan Zhang · Xiaodong Zhou

Received: 10 December 2009 / Accepted: 22 February 2010 / Published online: 9 March 2010

Abstract Localized surface plasmon resonance (LSPR) has been extensively studied as potential chemical and biological sensing platform due to its high sensitivity to local refractive index change induced by molecule adsorbate. Previous experiments have demonstrated the LSPR generated by gold nanoholes and its biosensing. Here, we realize large uniform area of nanoholes on scale of cm^2 on glass substrate by nanosphere lithography which is essential for mass production. The morphology of the nanoholes is characterized using scanning electron microscope and atomic force microscope. The LSPR sensitivity of the nanoholes to local refractive index is measured to be 36 nm/RIU. However, the chip has demonstrated high sensitivity and specificity in biosensing: bovine serum albumin adsorption is detected with LSPR peak redshift of 27 nm, and biotin-streptavidin immunoassay renders a LSPR redshift of 11 nm. This work forms a foundation toward the cost-effective, high-throughput, reliable and robust chip-based LSPR biosensor.

Keywords Localized surface plasmon resonance (LSPR) · Nanosphere lithography (NSL) · Nanohole · Nanoparticles · Biosensing

G. Xiang
School of Physical & Mathematical Sciences,
Nanyang Technological University, 21 Nanyang Link,
Singapore 637371, Singapore

N. Zhang · X. Zhou (✉)
Institute of Materials Research and Engineering, A*STAR (Agency for Science, Technology and Research), 3 Research Link, Singapore 117602, Singapore
e-mail: donna-zhou@imre.a-star.edu.sg

Introduction

Localized surface plasmon resonance (LSPR) is coherent oscillation of conduction electrons confined in noble metallic nanoparticles which is excited by electromagnetic radiation [1–3]. LSPR causes two notable results that can be exploited: first, the strong extinction band (absorption and scattering) which can be used as chemical and biological molecular sensing platform [2]; second, the strong electromagnetic field near the surface of nanoparticles which is the basis for all surface-enhanced spectroscopic methods such as surface-enhanced Raman spectroscopy (SERS) [4]. The potential of LSPR as biosensing platform relies on the fact that the resonance frequency and intensity of LSPR are highly sensitive to the material, shape, size and local dielectric constant of the metal nanoparticles [5, 6]. The resonance frequency and sensitivity of LSPR is tunable by nanoparticles, and molecular adsorption or chemical bonding onto the nanoparticles causes additional resonance frequency shift which can be detected by extinction peak shift in optical transmission spectrum of the nanoparticles. Biosensing of silver nanotriangle arrays, fabricated by closely packed nanosphere lithography, has already been extensively studied [7, 8]. However, by the limit of small defect-free area on scale of μm^2 and instability of silver, the realization of a feasible biosensing device based on silver triangle array is difficult. Recently, LSPR biosensing based on gold nanoholes has been reported, either with randomly distributed [9–11] or periodically arranged nanoholes [12–14].

In this paper, large uniform area of gold nanoholes in cm^2 scale are fabricated on glass substrate by nanosphere lithography (NSL), in contrast to the smaller area of nanoparticles obtained by closely packed NSL. The morphology of the nanoholes is characterized using scanning

electron microscope (SEM) and atomic force microscope (AFM), and the LSPR sensitivity of nanoholes to local refractive index is measured. Detection of bovine serum albumin (BSA) binding and biotin-streptavidin immunoassay to gold nanoholes are realized, with LSPR extinction peak red-shifts 4-fold higher than the previously reported nanohole experiments in BSA test [10]. The detection of specific biotin–streptavidin bonding demonstrates that the LSPR peak shifts 11 nm after 21.3 fMol of effective streptavidin molecules are bonded onto the biotin functionalized nanoholes, this detectable streptavidin quantity is comparable to silver triangles [7], and the sample is reusable after removal of the anchored biotin.

Materials and Experiments

In our experiments, polystyrene (PS) nanospheres were purchased from Duke Scientific Ltd, biotinylated thiol was a gift from Max Planck Institute for Polymer Research in Germany, and other chemicals were purchased from Sigma–Aldrich.

A 4″ glass wafer was pre-treated with silicon ion implantation to introduce electrical charges on the glass surface for dispersing the nanospheres, then it was cleaved into 7.5 mm × 10 mm chips as substrates by Disco dicing saw. Glass substrates were cleaned by sonication in acetone for 5 min followed by DI water rinse and nitrogen gas blow-dry. Prior to deposition of PS nanospheres, the substrates were drop coated by PDDA of 2 wt%, rinsed by DI water and blow-dried by nitrogen gas. The gross electrostatic force resulted from PDDA, implanted silicon ions and PS nanospheres balances the capillary force of nanospheres, avoiding them from forming close-packed or clustered defects. Afterwards, 110-nm diameter nanospheres of 0.1% in water were drop coated and evenly dispersed onto the substrates. Gold film was perpendicularly deposited onto the substrates with nanospheres at a rate of 1 Å/s by a R-Dec thermal evaporator, and a substrate without nanospheres was deposited in the same batch and served as a reference to LSPR spectral measurement. The gold deposition thickness was 40 nm, monitored by a microbalance. The nanospheres were then removed by sonication in water for 40 s, and nanoholes were successfully fabricated. The morphology of the nanoholes was characterized by a JEOL 6700 SEM at an acceleration voltage of 5 kV and a Digital Image AFM in tapping mode.

LSPR extinction spectra were measured using an Ocean Optics fiber spectrometer with a wavelength range of 200–900 nm and a resolution of 0.33 nm. The spectrometer defines the extinction spectrum as $S = -\log\left(\frac{I_s - I_d}{I_r - I_d}\right)$, where I_s, I_r and I_d are respectively the light intensities of the sample, reference and dark noise. The UV–Vis light from the deuterium and halogen source was coupled to an optical fiber, transmitted through the sample, and collected by another fiber to the spectral analyzer. Two 74-UV collimating lenses were respectively used to collimate the light from the illuminating fiber to a 5-mm diameter spot and focus it back into the collecting fiber.

Results and Discussions

Morphology of Nanoholes

SEM images of 110 nm randomly dispersed nanoholes fabricated on the glass substrate are presented in Fig. 1a, b. It is found that the substrate is almost entirely distributed with nanoholes without defect. The average interval of the nanoholes is 2 times of the diameter, which implies there maybe some plasmonic coupling between the nanoholes, and this needs further study. Figure. 1c is the AFM image of the nanoholes. The cross-section of the nanoholes indicates a diameter of 125 nm and a depth of 39 nm, which are consistent with our process setting. We notice the nanohole's cross-section is not a square but a slope, as the capillary force attracted gold atoms to deposit under the PS nanospheres during gold evaporation. Such a profile is different from previously reported nanoholes [10, 11], and it benefits the bonding of more biomolecules in the plasmonics enhanced area.

LSPR Sensitivity and Experimental Control

In order to study the sensitivity of the nanoholes to local refractive index change, the LSPR extinction spectrum of a nanohole sample in air was measured, with the gold thin film substrate in air as a reference. Afterwards, LSPR extinction spectrum of the same sample in water was measured with the thin film substrate in water as reference. The LSPR spectra of the nanoholes in air and water, as well as their mean values and error bars (based on standard deviation), are shown in Fig. 2a, b. Since the nanoholes are evenly distributed in a large area of the substrate, in all experiments, changing the location of the light spot on the sample did not show noticeable difference in LSPR spectra. So in our experiments, the LSPR peak wavelengths were obtained by calculating the mean value of the peak wavelengths at different locations of the sample.

Strong resonance peak was observed at an averaged wavelength of 574.5 nm in air, which is consistent with literature [9]. The peak shifted 12-nm, to 586.3 nm in average, after the medium was changed to water. With 1.33 as the refractive index of water, the LSPR sensitivity of the nanoholes is calculated to be 36 nm/RIU. The lower

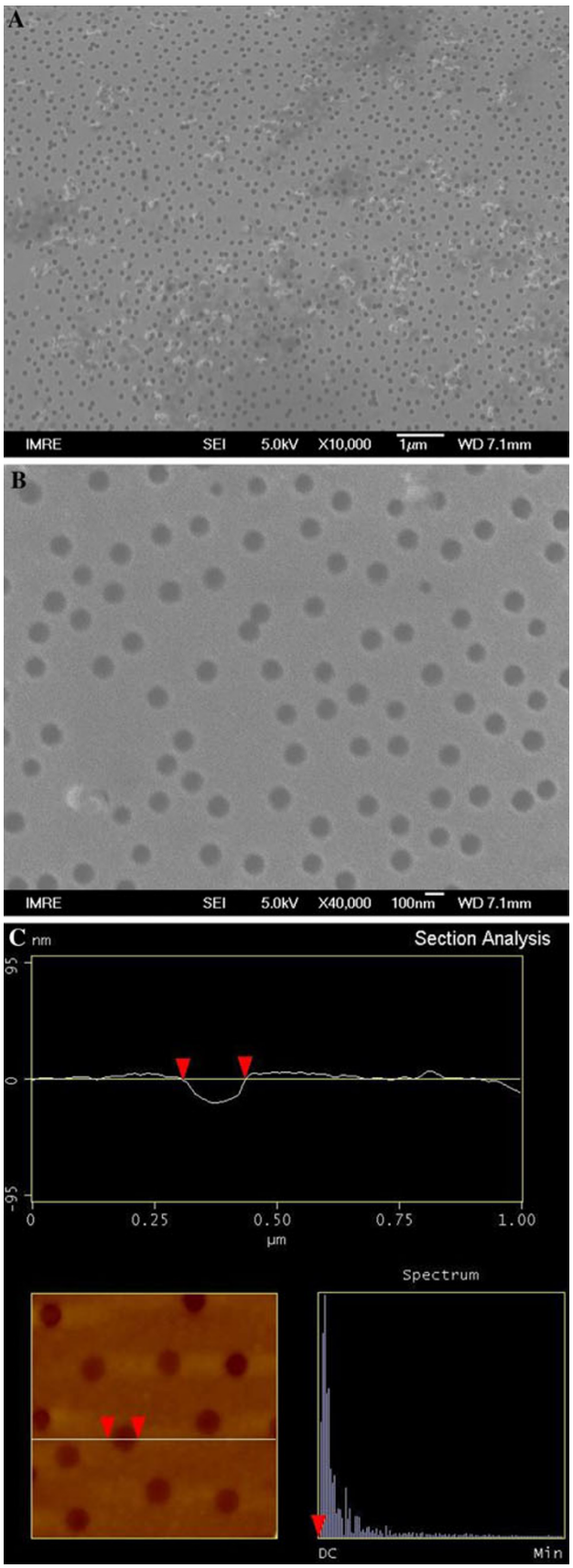

◀ **Fig. 1** SEM and AFM images of 110-nm gold nanoholes. **a** is the SEM image, **b** is a magnified photo of **a**, and **c** shows the AFM image and the cross-section of the nanoholes. The *scale bars* in **a** and **b** are 1 and 100 nm, respectively

sensitivity compared to 100 nm/RIU for 110-nm diameter nanoholes in Ref. [9] is due to the lower aspect ratio of our nanoholes, as the gold is thicker in our samples.

Before studying with BSA adsorption and biotin–streptavidin immunoassay, LSPR extinction spectra of nanoholes after incubation in water, ethanol and phosphate-buffered saline (PBS) were measured respectively as control experiments, and no extinction spectra change was observed before and after the incubation of these kinds of solvent. Therefore, we exclude the influence of the solvent on LSPR in the following BSA and streptavidin (SA) detections.

BSA Adsorption

For the investigation of BSA binding onto the nanoholes, the LSPR spectrum of a nanohole sample was first measured. Then, the sample was incubated with BSA in PBS buffer at the concentration of 1 mg/ml for 20 h at room temperature. The sample was nitrogen dried without rinse, and the LSPR extinction spectrum was measured. Afterwards, the sample was rinsed with PBS and water repeatedly and nitrogen dried and LSPR spectrum measured.

The detection of BSA adsorption was demonstrated as drawn in Fig. 3. Before BSA incubation of the nanohole sample, the LSPR peak of the bare nanoholes was measured to be 571 nm. After incubation in BSA in PBS, the peak shifted to 598 nm and indicated a 27-nm redshift. Since BSA has no selective absorption in UV–Vis region, this peak shift came from the nanohole LSPR in response to its local dielectric change induced by BSA, which physically adsorbed to the gold surface and the glass surface inside the nanoholes. As the plasmonic field is concentrated around the circumference of the nanoholes, it is mainly the BSA proteins adsorbed onto these areas caused the peak shift, and we estimate multilayer of BSA molecules accumulated on the surface. After subsequent rinsing with PBS, ethanol and DI water, it is found that the LSPR peak returned to 579.5 nm, and further sonication made the average wavelength of the sample down to 575 nm, very close to the wavelength before BSA adsorption. This confirms that the LSPR peak redshift was due to the physical adsorption of BSA molecules. The rinse and sonication of the sample did not bring the LSPR extinction peak back to its original position, due to the incomplete removal of BSA. After sonication, the standard deviation of the peak wavelengths for the measurements at different

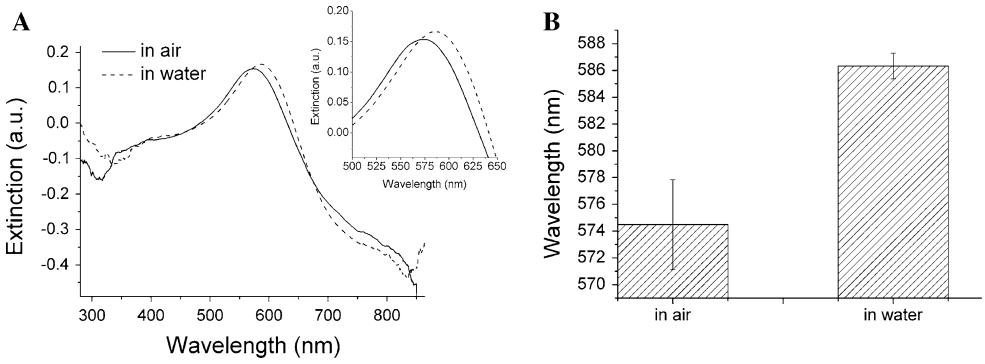

Fig. 2 LSPR extinction spectra of nanoholes in air and water (**a**), and their mean values and standard deviations of several measurements at different locations of the sample (**b**)

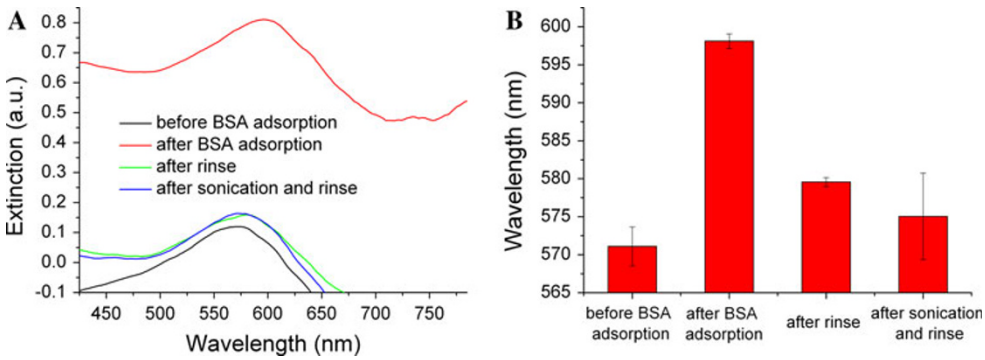

Fig. 3 Extinction spectra of BSA detection (**a**) and *error bars* of several measurements at different locations of the sample (**b**)

locations was high, indicated that BSA was removed more thoroughly at some areas than other locations.

We also noticed the strong intensity increase after BSA adsorption. However, we avoid using intensity as the indicator of signal detection because light intensity is sensitive to many factors.

Our BSA test has 4 times more LSPR wavelength shift than the nanoholes in Ref. [10], while their bulk reflective index sensitivity is 110 nm/RIU, i.e., 3 times higher than ours. Besides the influences come from different nanohole size, thickness and distribution, we believe the shape of our nanoholes is more beneficial for BSA bonding, as our nanoholes are in cone shape, and thus larger BSA-adsorbed areas are covered with electromagnetic field. Same explanation applies to the following biotin–streptavidin experiment, in which the detectable streptavidin is comparable to silver nanotriangles [7].

Biotin-Streptavidin Immunoassay

To investigate the specificity and adhesion of analyte to the surface of nanoholes, biotin–streptavidin immunoassay was studied with a nanohole sample in several subsequent steps, and the LSPR spectrum was taken after each step. First, the sample was immersed into biotinylated thiol at the concentration of 374 μM in ethanol for 20 h at room temperature to form a self-assembled monolayer of biotin, then the sample was rinsed with ethanol and DI water and nitrogen dried. Second, the sample was immersed into 1 μM streptavidin in PBS for 20 h at room temperature, dried without rinse. Third, the sample was rinsed repeatedly with ethanol, PBS and DI water and nitrogen dried. Fourth, the sample was exposed under a UV cleaner for 30 min to break the chemical bond between the thiol and gold, then the sample was rinsed with ethanol, PBS and DI water repeatedly and nitrogen dried. Fifthly, the sample was incubated with biotinylated thiol in ethanol for 20 h at room temperature again, rinsed and dried.

For the biotin-streptavidin immunoassay, its LSPR extinction spectra are plotted in Fig. 4. The nanohole sample modified with biotin had an LSPR peak at 567 nm. After incubation in streptavidin and drying, the LSPR peak redshifted to 578 nm and exhibited a prominent 11-nm shift, due to the local dielectric change induced by streptavidin bonding. Repeated rinse of ethanol, PBS and DI water only blueshifted the wavelength 3 nm, because some unspecific bonded substances on the sample were washed away. This is in contrast to BSA detection in which the rinse brought its LSPR peak back, because the streptavidin is chemically bonded to the biotin functionalized surface of nanoholes rather than the physical adsorption of BSA. Biotin and streptavidin were supposed to be bonded only on gold, and the LSPR peak shift was mainly contributed from the streptavidin at the circumference of the nanoholes. As the density of our nanoholes was about 3/μm^2, the area illuminated by the detection light was 5 mm in

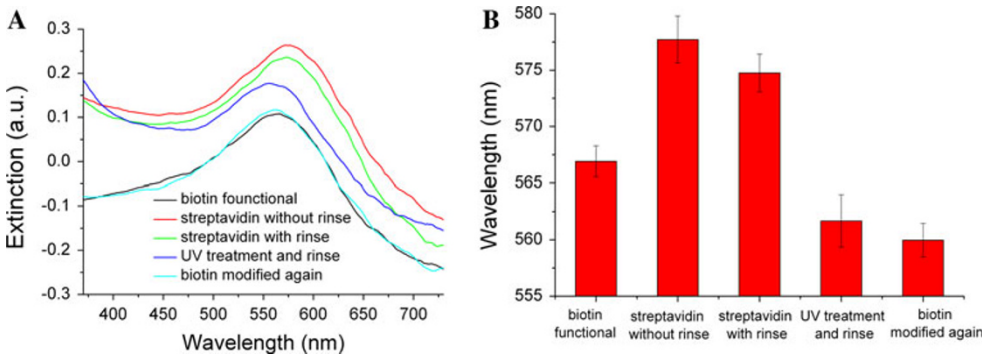

Fig. 4 Extinction spectra biotin–streptavidin immunoassay (**a**), and *error bars* for the LSPR peaks at different locations of the sample (**b**)

diameter, based on the size/shape of the nanohole and streptavidin (SA) [7], there were about 218 SA around each nanohole; therefore, the effective number of streptavidin under detection for a sample was estimated to be 1.28×10^{10}, i.e., 21.3 fMol/sample. This is about 3 times of the limit of detection (LOD) reachable by silver nanotriangles measured in nitrogen gas environment, where 4.6×10^{9} SA/sample, equivalent to 7.6 fMol/sample, was reported by Northwestern University [7]. After UV exposure and rinse, the LSPR peak turned to 561.7 nm. This was expected as the UV exposure broke the bond between biotinylated thiol and gold. No obvious extinction intensity change at this step was observed, which inferred the biotin and streptavidin were not washed away although they were not bonded on the nanoholes and were already out of the localized plasmonic field of 5–15 nm high from the metal surface. When we incubated the UV-exposed sample again with biotinylated thiol in ethanol, extinction intensity reduced, and wavelength of the sample's LSPR extinction peak returned to an even lower wavelength of 560 nm, because the streptavidin nearby the nanoholes were dragged away by excessive biotin in ethanol, and a new layer of biotin was anchored onto the sample. This means the sample is reusable in our experiments, thus the cost of the device can be further reduced.

Conclusion

In summary, we successfully fabricated uniform gold nanoholes in a large area (>cm^2) of glass substrate, and characterized the morphology and the LSPR prosperities of the nanoholes. Although these nanoholes have lower sensitivity to refractive index compared to reported experiments in literatures, a higher sensitivity to biochemical molecules was demonstrated by this device due to the cone shape of the nanoholes. The nonspecific BSA binding demonstrated 4 times more wavelength shift than reported nanoholes. In biotin–streptavidin test, 21.3 fMol of effective streptavidin manifested a 11-nm wavelength redshift, this sensitivity seems satisfactory because 7.6 fMol of streptavidin is the calculated LOD of the LSPR sensor with silver nanotriangles. Since our research is based on gold and glass substrate, and the nanoholes are evenly distributed on a large glass area, our study proves the great potential for such a cost-effective and robust chip to become a specific and reliable biosensor.

Acknowledgments We acknowledge the financial support of Institute of Materials Research and Engineering (IMRE) in Singapore on localized surface plasmon resonance (LSPR) project IMRE09/1C0420, and we thank Ms Christina TAN Yuan Ling in IMRE, A*STAR for taking the SEM images.

References

1. C.F. Bohren, D.R. Huffman, *Absorption and Scattering by Small Particles* (Wiley Interscience, New York, 1983)
2. E. Hutter, J.H. Fendler, Adv. Mater. **16**, 1685 (2004)
3. B. Sepulveda, P.C. Angelome, L.M. Lechuga, L.M. Liz-Marzan, Nano Today **4**, 244 (2009)
4. M. Fleischmann, P.J. Hendra, A.J. Mcquillan, Chem. Phys. Lett. **26**, 163 (1974)
5. S. Underwood, P. Mulvaney, Langmuir **10**, 3427 (1994)
6. P. Mulvaney, Langmuir **12**, 788 (1996)
7. A.J. Haes, R.P. Van Duyne, J. Am. Chem. Soc. **124**, 10596 (2002)
8. J.C. Riboh, A.J. Haes, A.D. McFarland, C.R. Yonzon, R.P. Van Duyne, J. Phys. Chem. B **107**, 1772 (2003)
9. J. Prikulis, P. Hanarp, L. Olofsson, D. Sutherland, M. Käll, Nano Lett. **4**, 1003 (2004)
10. D. Gao, W. Chen, A. Mulchandani, Appl. Phys. Lett. **90**, 073901 (2007)
11. T. Rindzevicius, Y. Alaverdyan, A. Dahlin, F. Höök, D.S. Sutherland, M. Käll, Nano Lett. **5**, 2335 (2005)
12. R. Gordon, D. Sinton, K.L. Kavanagh, A.G. Brolo, Acc. Chem. Res. **41**, 1049 (2008)
13. A. De Leebeeck, L.K.S. Kumar, V. De Lange, D. Sinton, R. Gordon, A.G. Brolo, Anal. Chem. **79**, 4094 (2007)
14. J. Jin, J.G. O'Connell, D.J.D. Carter, D.N. Larson, Anal. Chem. **80**, 2491 (2008)